



Study on interaction between the 2-(2-phenylethyl)-5-methylbenzimidazole and dsDNA using glassy carbon electrode modified with poly-3-amino-1,2,4-triazole-5-thiol

Gözde Aydoğdu Tığ^{a,*}, Gülenem Günendi^a, Tuğba Ertan Bolelli^b, İsmail Yalçın^b, Şule Pekyardımcı^a

^a Faculty of Science, Department of Chemistry, Ankara University, Ankara 06100, Turkey

^b Faculty of Pharmacy, Department of Pharmaceutical Chemistry, Ankara University, Ankara 06100, Turkey

ARTICLE INFO

Article history:

Received 15 April 2016

Received in revised form 20 June 2016

Accepted 21 June 2016

Available online 24 June 2016

Keywords:

Benzimidazole

dsDNA biosensor

3-amino-1,2,4-triazole-5-thiol

Differential pulse voltammetry

Molecular docking

ABSTRACT

In this study, we developed an electrochemical DNA biosensor based on a poly-3-amino-1,2,4-triazole-5-thiol (P(AT)) film modified glassy carbon electrode (GCE/P(AT)). For the first time, this electrode was used for the determination of a new benzimidazole molecule, 2-(2-phenylethyl)-5-methylbenzimidazole (BNN-17). The electrochemical behavior of the GCE/P(AT) electrode was investigated using cyclic voltammetry (CV) and electrochemical impedance spectroscopy (EIS). Differential pulse voltammetry (DPV) was carried out to obtain the change in the oxidation signals of the guanine and adenine before and after interaction with the BNN-17. Under the optimum conditions, a linear dependence of the guanine oxidation signals was observed when the BNN-17 concentration was in the range of 0.213–32.03 $\mu\text{mol L}^{-1}$ ($R^2 = 0.991$). The limit of detection (LOD) and limit of quantification (LOQ) were found to be 0.063 $\mu\text{mol L}^{-1}$ and 0.21 $\mu\text{mol L}^{-1}$, respectively. The influence of potential interfering substances on BNN-17 determination was studied. Finally, the GCE/P(AT)/dsDNA electrode was utilized for the determination of BNN-17 in serum samples which gave sensitive, accurate, and precise results. The binding mode of BNN-17 with dsDNA was investigated using DPV, UV–vis absorption spectroscopy, and molecular docking methods. All of the experimental results indicated that BNN-17 preferred to bind on the minor groove of dsDNA. The results obtained from the experimental data were in good agreement with the molecular docking studies.

© 2016 Elsevier B.V. All rights reserved.

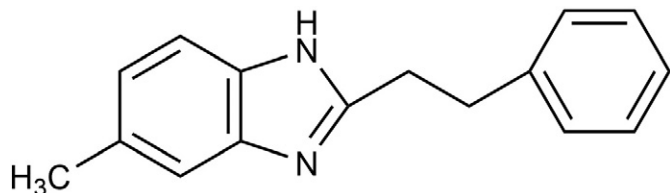
1. Introduction

Benzimidazole derivatives represent an important pharmacophore and privileged structure in medicinal chemistry due to their broad spectrum of biological activity [1]. They have attracted significant attention as an important class of heterocyclic compounds in the field of chemotherapy and other types of cancer treatment. Due to these properties, benzimidazole derivatives have received great interest in connection with their synthesis in recent years [2]. Furthermore, benzimidazole derivatives are structural isoesters of naturally occurring nucleotides, thus they can interact with biological macromolecules such as proteins, enzyme receptors, and nucleic acids [3]. Several anticancer agents in clinical use have been shown to be potent inhibitors of DNA topoisomerases. Molecular studies have shown that topoisomerase II

has a range of critical roles, including some related to DNA replication and transcription. Most clinically active drugs that target topoisomerase II generate enzyme-mediated DNA damage. Previous studies have promised a more refined ability to target topoisomerase II as an effective anticancer strategy [4–6]. In recent years, detailed investigations of bi- and ter-benzimidazole derivatives revealed that these compounds constitute a new class of DNA topoisomerase I and II inhibitors. Work on such compounds indicates that a fused ring system in the structure is critical for the activity [7–11]. Single-strand DNA breaks in the presence of topoisomerase I, which is induced by the minor groove binding drugs being highly site specific. It has been reported that the bisbenzimidazole derivatives Hoechst 33258 and 33342 strongly inhibit the catalytic activity of topoisomerase I by binding with high affinity into the minor groove of AT-rich sequences of double-helical DNA [12,13]. A number of benzimidazole derivatives which were synthesized by our group were found to be inhibitors of topoisomerase I and II [14]. Herein, some further studies on 2-(2-phenylethyl)-5-methylbenzimidazole (BNN-17, see Scheme 1), which is one of the synthesized compounds,

* Corresponding author.

E-mail address: gaydogdu@science.ankara.edu.tr (G.A. Tığ).



Scheme 1. The structure of 2-(2-phenylethyl)-5-methylbenzimidazole (BNN-17).

were performed to investigate the interaction between the compound and dsDNA.

Recently, more attention has been paid to the development of DNA biosensors to provide new techniques for rapid and sensitive detection of pathogens [15], human genetic diseases [16], and DNA–drug interactions [17,18]. DNA biosensors are generally based on electrodes with oligonucleotide immobilization. For this purpose, conducting polymers and/or their composites were widely used due to their promising electronic, optoelectronic, and electrochemical properties, which can be simply designed and fabricated and then applied in electronic devices [19–21]. Many conducting polymers, such as polyaniline, polypyrrole, polythiophene, poly(*p*-phenylene), and poly(3,4-ethylenedioxythiophene) have been widely used as the immobilizing substrate for biomolecules especially enzymes, proteins, or nucleic acids because of their high conductivity and high redox reversibility [22]. Recently, poly-3-amino-1,2,4-triazole-5-thiol (P(AT)) has been used due to its various favorable properties, such as low molecular weight, stability, selectivity, and homogenous film coating with controllable thickness [23]. This polymer has been used for the detection of the *L*-dopa/*L*-tyrosine ratio, which is an electrochemical marker for metastatic malignant melanoma [24] and uric acid [25]. Moreover, this polymer has functional groups ($-\text{NH}_2$, $-\text{SH}$) that would be beneficial to the immobilization of biomolecules such as nucleic acids.

In the present study, we developed an electrochemical dsDNA biosensor based on a GCE modified with P(AT) film (GCE/P(AT)). The GCE/P(AT)/dsDNA electrode was prepared by the adsorption of dsDNA on the P(AT) coat on the GCE. For the first time, the developed dsDNA biosensor was employed for the electrochemical determination of BNN-17. The P(AT) film was characterized by cyclic voltammetry (CV), electrochemical impedance spectroscopy (EIS), and scanning electron microscopy (SEM) techniques. The experimental conditions, such as the dsDNA concentration, adsorption time, BNN-17 concentration, and its interaction time with the dsDNA, were optimized. Moreover, the interaction mechanism between the dsDNA and the BNN-17 was examined by differential pulse voltammetry (DPV), UV–vis spectroscopy, and molecular docking techniques. Furthermore, this procedure was also applied to determine the concentration of BNN-17 in human serum samples with accurate, sensitive, and precise results.

2. Experimental

2.1. Chemicals

3-Amino-1,2,4-triazole-5-thiol (AT) was purchased from Aldrich. dsDNA (fish sperm) was obtained from Serva Company (Germany). 2-(2-phenylethyl)-5-methylbenzimidazole (BNN-17) was synthesized according to the literature [26,27]. Sodium acetate and acetic acid were purchased from Sigma–Aldrich. All other chemicals were of analytical grade. The solution of dsDNA (1 mg/1 mL) was prepared in ultrapure water and stored at $-20\text{ }^\circ\text{C}$. More diluted dsDNA solutions were prepared with 0.5 mol L^{-1} acetate buffer (pH 4.8) containing 0.02 mol L^{-1} NaCl. Stock solutions of BNN-17 (100 mg L^{-1}) were prepared in ethanol solution (70%). Working standard solutions were prepared daily by the appropriate dilution of the stock solution.

2.2. Apparatus

The electrochemical measurements were carried out using an AUTOLAB-PGSTAT 302N electrochemical analysis system (potentiostat/galvanostat combined with FRA2.0 module) (Eco Chemie, Utrecht, The Netherlands) connected to a three-electrode cell stand (Bioanalytical Systems, BAS, Inc., USA). A conventional three-electrode cell containing an Ag/AgCl (3 mol L^{-1} NaCl, BAS MF 2052) reference electrode, a platinum wire (BAS MW 1034) counter electrode, and bare (BGCE) or modified GCE as the working electrode was used. All experiments were performed in a standard one-compartment three-electrode cell with 10 mL capacity. The cyclic voltammograms (CVs) and differential pulse voltammograms (DPVs) were analyzed using the NOVA 1.11 software (ECO Chemie).

The pH values of the buffer solutions were measured using an ORION Model 1906 D. 720A pH/ion meter (Thermo Scientific, USA). Ultrapure water ($18.2\text{ M}\Omega\text{cm}$) from a Purelab Elga system (Veolia Water Systems Ltd., UK) was used for preparing all solutions. All measurements were carried out at room temperature.

UV–visible absorption spectra were measured with a Shimadzu 1700 (Pharma Spec) double beam spectrophotometer (Shimadzu Corporation, Tokyo, Japan) equipped 1 cm quartz cuvettes at room temperature in the wavelength range of 200–400 nm. The absorption spectra were recorded for the free dsDNA and the BNN-17 and dsDNA solution for the calculation of the binding constant of the reaction occurring between BNN-17 and dsDNA.

The scanning electron micrographs of the P(AT) film were recorded with a FEI Quanta 400F Field-Emission Scanning Electron Microscope (FESEM, Tokyo, Japan). The surface of the P(AT) was coated with Au–Pd alloy under vacuum before the micrographs were recorded.

2.3. Molecular docking study

The crystal structure of the synthetic DNA dodecamer d(CpGpCpGpApApTpTpCpGpCpG) was retrieved from the Protein Data Bank (PDB ID: 1BNA) [28]. Accelrys Discovery Studio 3.5 (Discovery Studio 3.5, Accelrys Inc., 2012) software was used for the preparation and docking processes. The DNA was taken, water molecules were removed, hydrogens were added, and their positions were optimized using the all-atom CHARMM force field and the Adopted Basis set Newton Raphson (ABNR) method available in the Discovery Studio 3.5 protocol until the root mean deviation (RMS) gradient was $<0.05\text{ kcal/mol}/\text{\AA}^2$. The binding site was defined using the cavity finding method which was modified to accommodate the minor groove of DNA. The binding sphere for 1BNA (8.88, 24.72, 6.11, 8.95) was selected from the active site using the binding site tools. Our synthesized compound of BNN-17 was sketched; all-atom CHARMM force field parameterizations were assigned and then minimized using the ABNR method as described above. Conformational searches of the BNN-17 were carried out using a simulated annealing molecular dynamics (MD) approach. Afterwards, the CDocker [29] method was performed using Discovery Studio 3.5. The DNA was held rigid while the BNN-17 was allowed to flex during the refinement. Finally, all docked poses were scored by applying the Analyze Ligand Poses subprotocol and binding energies were calculated by applying the Calculate Binding Energy subprotocol in Discovery Studio 3.5 by using in situ ligand minimization step (ABNR method) and implicit solvent model (Molecular Mechanics–Generalized Born with Molecular Volume, GBMV). The lowest binding energy was taken as the best-docked conformation of the compound for the DNA.

2.4. Preparation of the modified electrode

Firstly, the surface of the GC electrode was polished with $0.05\text{ }\mu\text{m}$ alumina powder until a mirrored finish was obtained and then it was rinsed thoroughly with ultrapure water followed by ethanol. Then, sonication was used to remove the alumina residues, and it was dried at

room temperature. The GCE/P(AT) was prepared according to the literature [25]. Briefly, the P(AT) film was electrochemically deposited between -0.20 V and $+1.70$ V (vs. Ag/AgCl) at a scan rate of 50 mVs $^{-1}$ with 15 cycles in 0.1 mol L $^{-1}$ H $_2$ SO $_4$ containing 1.0 mmol L $^{-1}$ AT. Following this procedure, the GCE was covered with a thin film of P(AT). Then, the GCE/P(AT) was washed with ultrapure water and allowed to dry for 1 h at room temperature.

For the immobilization of the dsDNA, the GCE/P(AT) was immersed into vials containing 40 μ g mL $^{-1}$ dsDNA in a 0.5 mol L $^{-1}$ acetate buffer solution (0.02 mol L $^{-1}$ NaCl) for 15 min. Each of the electrodes was then gently rinsed with acetate buffer (0.5 mol L $^{-1}$ at pH 4.8) for 3 s for the removal of the unbound dsDNA at the modified electrode surface.

2.5. Interaction of BNN-17 with dsDNA

Electrochemical detection of the interaction between the BNN-17 and the dsDNA on the modified GCE is dependent on the oxidation signals of guanine. For this purpose, the GCE/P(AT)/dsDNA was immersed into a BNN-17 solution in 0.5 mol L $^{-1}$ acetate buffer (pH 4.8) for various times after the adsorption of the dsDNA onto the GCE/P(AT). The electrode was rinsed with acetate buffer after the interaction and then replaced in the BNN-17-free acetate buffer solution, where differential pulse voltammograms were recorded. The DPV studies were performed in the potential range of $+0.4$ to $+1.2$ V (vs. Ag/AgCl) in 0.5 mol L $^{-1}$ pH 4.8 acetate buffer solution containing 0.02 mol L $^{-1}$ NaCl. The DPV conditions used were as follows: step potential: 0.003 V; modulation amplitude: 0.05 V; modulation time: 0.02 s; interval time: 0.2 s; and scan rate: 0.015 Vs $^{-1}$.

2.6. Preparation of serum samples

Human serum samples supplied from healthy individuals were selected and stored at -20 °C until the assay procedure. 10 μ L volume of serum was transferred into a vial containing 90 μ L acetate buffer solution and a certain volume of the stock solution of BNN-17 was added into the vial. This mixture was transferred to an electrochemical cell and left to interact with the GCE/P(AT)/dsDNA electrode for 60 s. After the interaction, the GCE/P(AT)/dsDNA electrode was rinsed and placed in a blank ABS and the DPVs were recorded.

3. Result and discussion

3.1. Electrosynthesis of P(AT)

The electrosynthesis of P(AT) was performed in 0.1 mol L $^{-1}$ H $_2$ SO $_4$ using the CV technique. As can be seen in Fig. 1(a), the first cycle of the forward scan had three oxidation peaks at 0.56 (x), 1.19 (y), and 1.3 V (z) (curve 1), and in the reverse scan a reduction peak at 0.96 V was observed. In the second cycle, the oxidation peak currents decreased and the oxidation peaks of a, b, and c were shifted to less positive potentials (curve 2). In the subsequent cycles, the oxidation peak currents increased concurrently (curve 15), which suggests that the new monomer undergoes oxidation in each oxidative potential scan and the amount of electroactive polymer increases on the GCE [25].

3.2. SEM images of bare GCE and P(AT) modified electrodes

SEM micrographs of the bare GCE and P(AT)-coated GCE are shown in Fig. 1. As shown in Fig. 1(c,d), the surface morphology of the P(AT)-coated GCE was different from that of the bare GCE (Fig. 1(b)). The bare GCE presented a more uniform and smooth structure, whereas the P(AT) film exhibited a rough surface. This confirmed that the surface of the GCE was covered with P(AT) and a thin P(AT) film was formed on the GCE. As shown in Fig. 1(e), a heterogeneous layer on the polymer surface was observed after immobilization of dsDNA. To further confirm the immobilization of dsDNA on polymer film, the

energy dispersive X-ray spectroscopy (EDS) analysis was conducted and the spectrum was shown in Fig. 1(f). The signals of C and N elements in EDS data confirm the existence of P(AT) on GCE surface and the P signal indicates the successful immobilization of dsDNA upon the surface of the GCE/P(AT) (Fig. 1(f)). The presence of ionic chloride and sodium due to the preparation of dsDNA solution in acetate buffer containing NaCl.

3.3. Electrochemical characterization of P(AT) and P(AT)-DNA-modified GCEs

To investigate the electron transfer properties of bare, GCE/P(AT), and GCE/P(AT)/dsDNA, ferro-ferricyanide ion (Fe(CN) $_6^{3-/4-}$) was used [30]. The CV and EIS techniques were utilized for the electrochemical characterizations of the BGCE, GCE/P(AT), and GCE/P(AT)/dsDNA electrodes in 0.1 mol L $^{-1}$ KCl containing 5.0 mmol L $^{-1}$ Fe(CN) $_6^{3-/4-}$. Fig. 2(A) shows the CVs of the bare and modified GCEs at a scan rate of 50 mV s $^{-1}$. The anodic and cathodic peak currents of the Fe(CN) $_6^{3-/4-}$ for P(AT)-coated GCE increased according to that of the BGCE. In addition, the peak-to-peak separations (ΔE_p) for BGCE and GCE/P(AT) electrodes were 0.301 and 0.142 V, respectively (Table S1). These results suggest that the positively charged P(AT) film electrostatically attracts Fe(CN) $_6^{3-/4-}$ ions with a negative charge [31]. When the surface of the GCE/P(AT) was covered with dsDNA (Fig. 2(A)(c)), a decrease in the peak currents of the redox probe was observed. Moreover, the ΔE_p increased (0.418 V) when compared to that of the P(AT) modified electrode. The results showed that the negatively charged dsDNA had been adsorbed on the surface of the GCE/P(AT), and this impedes the Fe(CN) $_6^{3-/4-}$ ions access to the surface of the GCE [32,33].

EIS was also used to investigate the electron transfer features of the bare and modified electrodes. Fig. 2B presents the Nyquist plots of the BGCE (curve a), GCE/P(AT) (curve b), and GCE/P(AT)/dsDNA (curve c) electrodes in 0.1 mol L $^{-1}$ KCl containing 5.0 mmol L $^{-1}$ Fe(CN) $_6^{3-/4-}$. The Nyquist plot shows a semicircle part at high frequencies and the diffusion control impedance of ions at low frequencies. The values of the electron transfer resistance (R_{et}) were calculated for BGCE, GCE/P(AT), and GCE/P(AT)/dsDNA as 2097 , 532 , and 1010 Ω , respectively. It is clear that the P(AT) film increases the rate of electron transfer at the solution/electrode interface when compared with the BGCE. After the adsorption of dsDNA to the surface of the P(AT) film, the R_{et} value of the GCE/P(AT)/dsDNA electrode increased due to the negative charge of the dsDNA [18].

3.4. Immobilization of dsDNA onto P(AT) modified GCEs

To obtain the best conditions for the electrochemical response of the GCE/P(AT)/dsDNA electrode, the adsorbed dsDNA concentration at the surface of the GCE/P(AT)/dsDNA electrode was optimized. Fig. 3 exhibits a plot of the guanine and adenine oxidation current signals as functions of the dsDNA concentration. As can be seen from the figure, the peak currents of guanine increased with increasing concentration of dsDNA up to 40 μ g mL $^{-1}$, and then became constant (Fig. 3 (A)). Thus, 40 μ g mL $^{-1}$ of the dsDNA was chosen as the optimum value for the determination of and interaction with BNN-17 in the subsequent experiments. The effect of the adsorption time of the dsDNA at the GCE/P(AT) surface was evaluated between 1 and 25 min. As shown in Fig. 3 (B), the oxidation peak currents of guanine increased up to 15 min of the adsorption time and then leveled off. Therefore, the optimum adsorption time was selected as 15 min.

3.5. Electrochemical studies for the interaction of BNN-17 with dsDNA at GCE/P(AT)

The effect of the concentration of the BNN-17 on the DPV signals in the presence of 40 μ g mL $^{-1}$ dsDNA was evaluated in the concentration range of 0.213 μ mol L $^{-1}$ and 85.40 μ mol L $^{-1}$. Fig. 4 displays the guanine

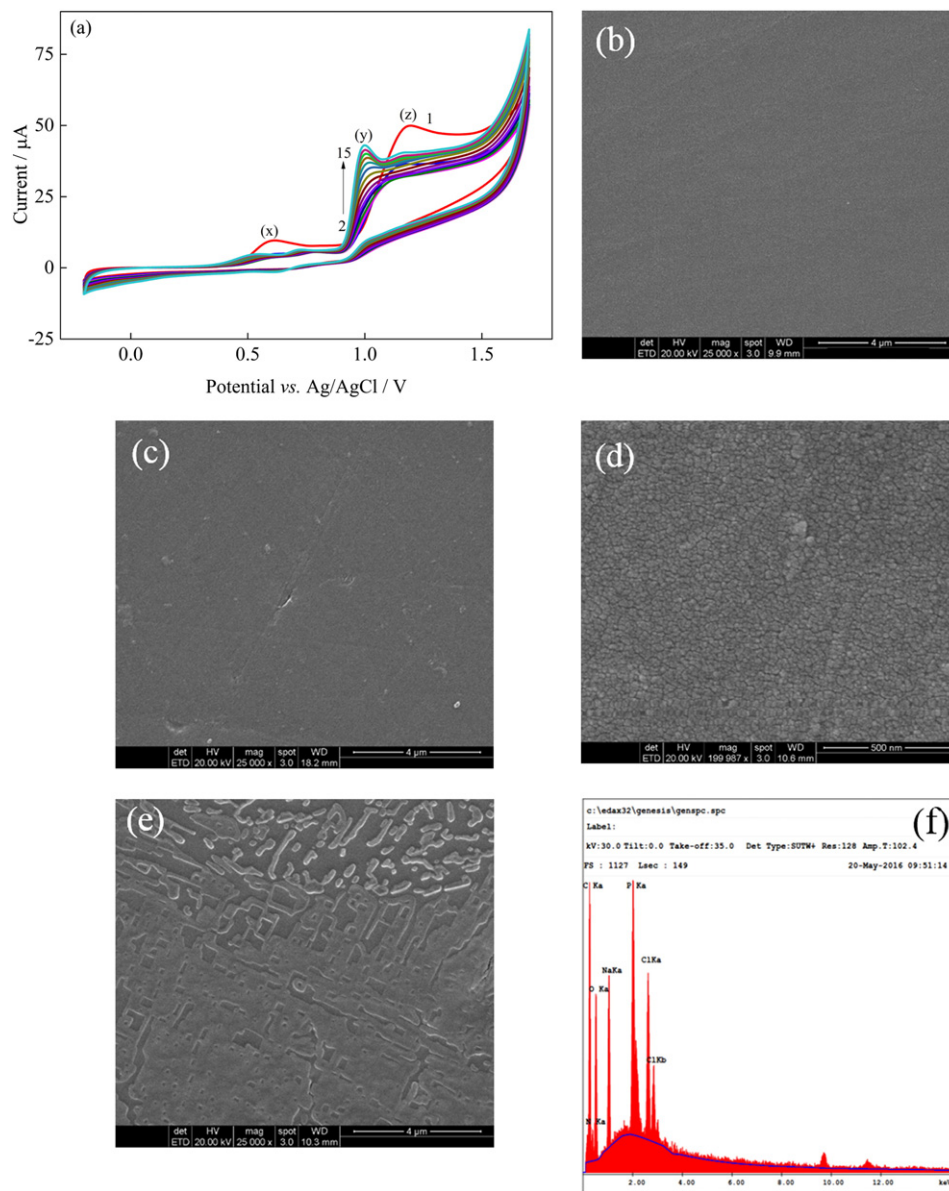


Fig. 1. Cyclic voltammograms recorded during the electroynthesis of P(AT) on the GCE in $0.1 \text{ mol L}^{-1} \text{ H}_2\text{SO}_4$ (a), SEM images of the bare GCE (b), GCE/P(AT) (c,d), and GCE/P(AT)/dsDNA (e), the EDS spectra of GCE/P(AT)/dsDNA (f).

and adenine oxidation signals at the GCE/P(AT) electrode for the different concentrations of BNN-17. Increasing the concentration of the BNN-17 caused a decrease in the oxidation peak current of the guanine and adenine which corresponds to the binding of the BNN-17 to those electroactive bases. This could be explained as possible damage to, or shielding of, the oxidizable groups of the electroactive bases while the BNN-17 interacts with dsDNA at the surface of the GCE/P(AT) [34,35].

It was expected that the binding of the BNN-17 to the dsDNA would be dependent on the interaction time. As shown in Fig. 5(A), the guanine peak currents decreased as the time increased up to 60 s, and then the currents almost leveled off. Thus, 60 s was selected as the optimum interaction time in all of the subsequent experiments.

As can be seen from Fig. 5(B), the oxidation peak currents for the guanine were linear with the BNN-17 concentration over the range of $0.213\text{--}32.03 \text{ } \mu\text{mol L}^{-1}$ with a linear equation of $I(\mu\text{A}) = -0.0103C + 0.418$ with $R^2 = 0.991$ ($n = 3$) where C is the BNN-17 concentration. The limit of detection (LOD) and limit of quantification (LOQ) from the calibration curve were found to be 0.063 and $0.21 \text{ } \mu\text{mol L}^{-1}$, respectively. The LOD and LOQ values confirmed the

sensitivity of the modified electrode which was calculated using the following equation [36]:

$$\text{LOD} = 3.3s/m, \text{ LOQ} = 10s/m \quad (1)$$

where s is the standard deviation of the current (three runs) for the lowest concentration of the linearity range, m is the slope of the related calibration curve. The analytical characteristics obtained for the BNN-17 determination using the DPV method are shown in Table 1.

The repeatability and reproducibility studies are the most important properties for biosensor application. The repeatability and reproducibility of the GCE/P(AT)/dsDNA electrode were evaluated by measuring the oxidation peak current of guanine after interaction with BNN-17. The repeatability for the same electrode was calculated from the relative standard deviation (RSD) of the guanine oxidation currents and it was found to be 2.15% ($n = 7$). In addition, the reproducibility for five different electrodes was tested and the RSD value was found to be 3.17% (Table 1).

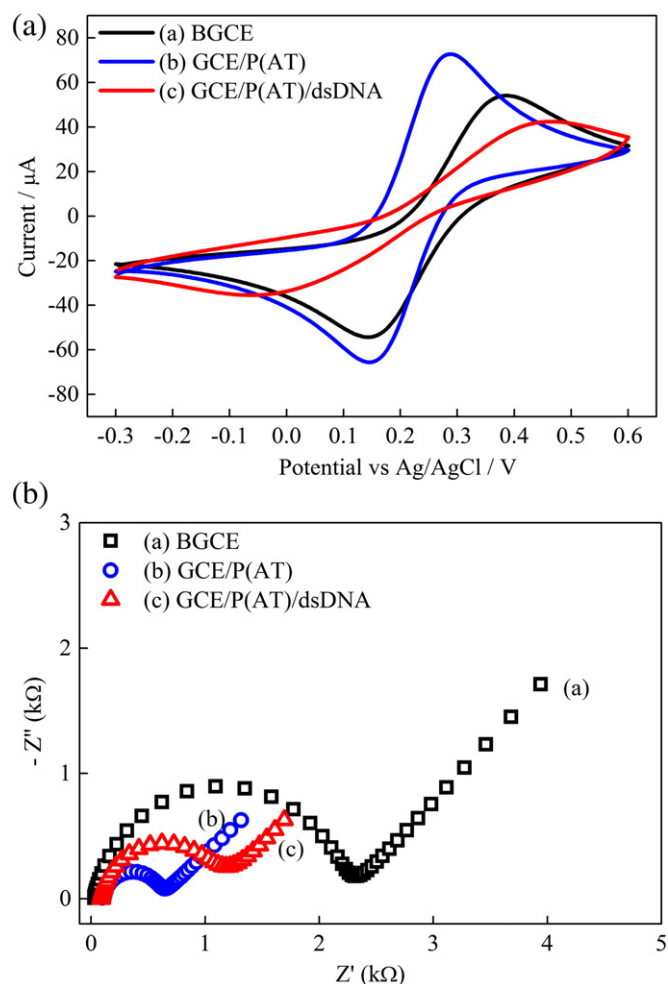


Fig. 2. (A) CVs of GCE, GCE/P(AT), and GCE/P(AT)/dsDNA electrode at scan rate of 50 mV s^{-1} ; (B) the Nyquist plots of (a) GCE, (b) GCE/P(AT), and (c) GCE/P(AT)/dsDNA in 0.1 mol L^{-1} KCl containing 5.0 mmol L^{-1} $\text{Fe}(\text{CN})_6^{3-/4-}$.

DNA–small molecule interactions involve intercalation, electrostatic interaction, and groove binding [37]. The electrostatic interaction mode happens out of the groove of the negative phosphate backbone of the dsDNA and, conversely, the intercalation and groove binding modes occur on the DNA double helix. DPV was used to determine the interaction mode between the dsDNA and the BNN-17. Generally, the positive shifts or negative shifts in the oxidation peak potential of the guanine showed the binding form to be via intercalation or electrostatic binding, respectively [38]. Since Fig. 4 clearly indicates no measurable shift in the oxidation peak potential of the guanine upon the addition of BNN-17, it can be concluded that the binding mode of the BNN-17 to the dsDNA was neither an electrostatic interaction nor intercalative binding. Furthermore, the decrease in the peak current of the dsDNA with the addition of the BNN-17 was due to the decrease in the equilibrium concentration of the free dsDNA. It can be assumed that a BNN-17–dsDNA complex (Eq. (2)) occurred between the dsDNA and BNN-17, and that this complex was electrochemically more inactive than the dsDNA.



If it is supposed that the interaction of the BNN-17 with the dsDNA generates only one complex, the interaction between the BNN-17 and dsDNA can be determined using the following equation [39,40]:

$$\log\left(\frac{1}{[\text{BNN-17}]}\right) = \log K + \log\left(\frac{I_{\text{BNN-17-dsDNA}}}{I_{\text{dsDNA}} - I_{\text{BNN-17-dsDNA}}}\right) \quad (3)$$

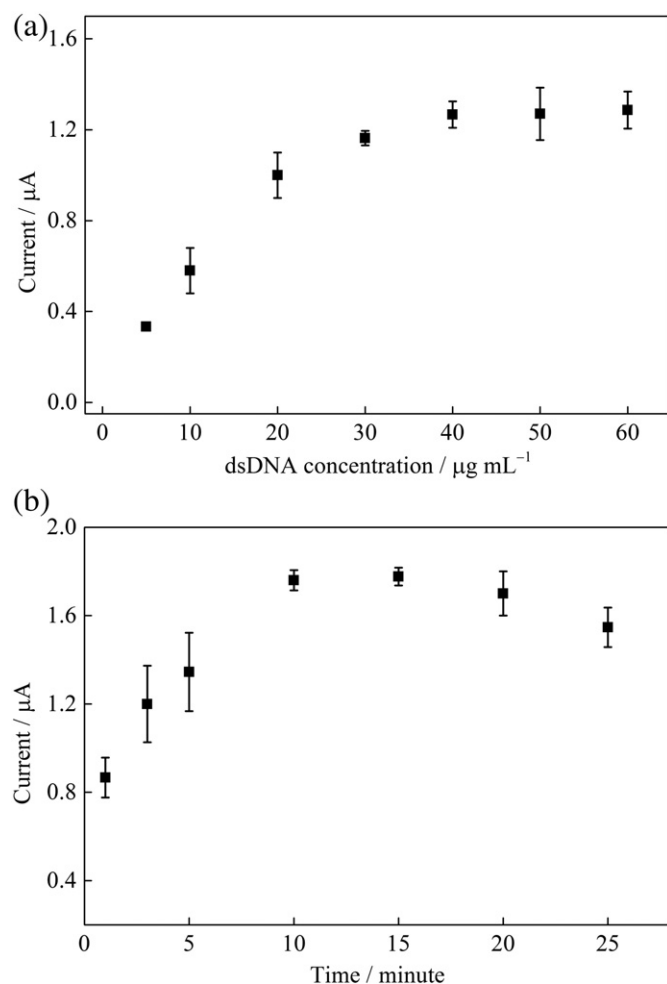


Fig. 3. The effect of dsDNA concentration (A) and adsorption time (B) on the electrochemical responses of guanine at GCE/P(AT)/dsDNA.

where K is the binding constant, I_{dsDNA} is the peak current of the dsDNA, and $I_{\text{BNN-17-dsDNA}}$ is the peak current of the BNN-17–dsDNA complex formation after the interaction of the drug with the dsDNA that is immobilized on the surface of the GCE/P(AT). The binding constant value of this complex, K , can be determined from the intercept of the non-linear curve fitting plot of $\log(1/[\text{BNN-17}])$ vs. \log

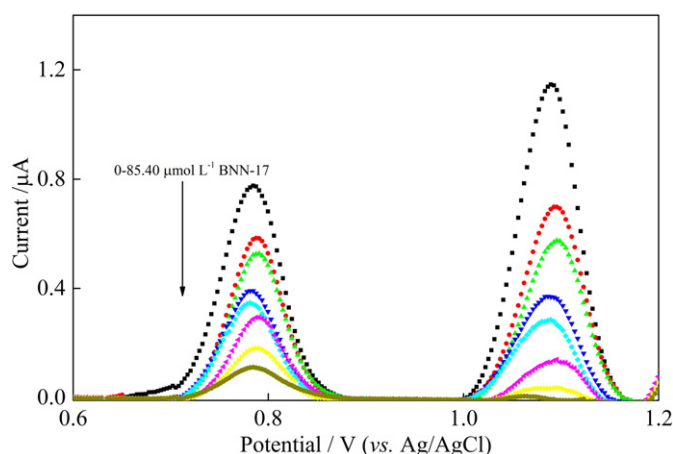


Fig. 4. DPVs of the guanine and adenine peaks in the absence and presence of the BNN-17 concentrations varying from 0.0 to $85.40 \mu\text{mol L}^{-1}$ in ABS (pH 4.8).

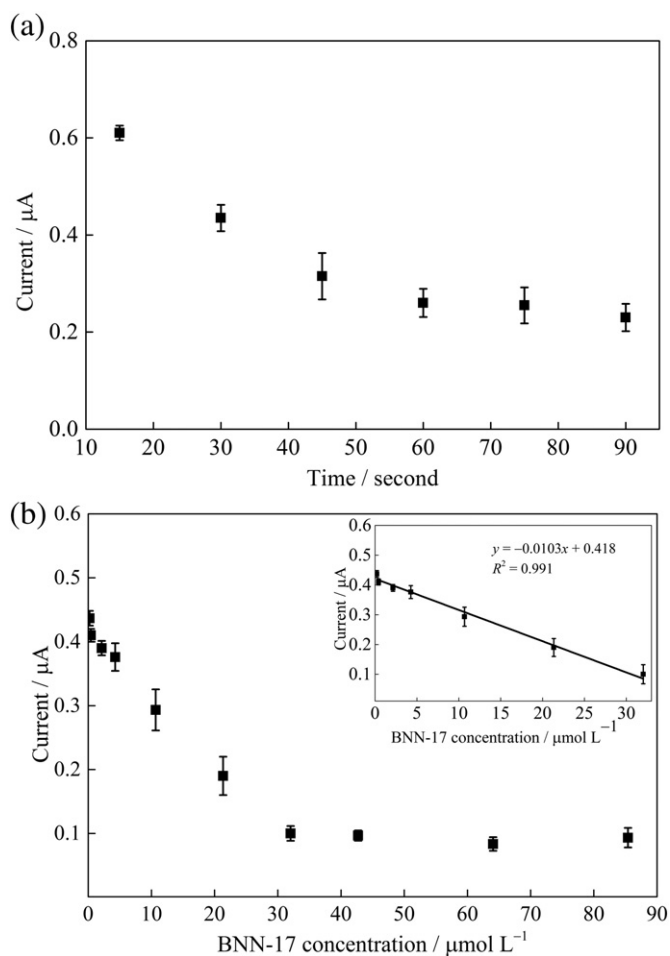


Fig. 5. (A) The effect of the interaction time and (B) concentration of BNN-17 with dsDNA on the guanine oxidation peak current (inset: linear dependence of BNN-17 concentration on the guanine signals at GCE/P(AT)/dsDNA electrode) (0.5 mmol L^{-1} ABS, pH 4.8).

$(I_{\text{BNN-17-dsDNA}}/I_{\text{dsDNA}} - I_{\text{BNN-17-DNA}})$. The value of K can be calculated as $2.9 \times 10^3 \text{ L mol}^{-1}$.

3.6. UV–vis spectrophotometric studies for the interaction of BNN-17 with dsDNA

To investigate the drug–DNA interaction, UV–vis absorption spectroscopy was also used. Generally, a bathochromic/hypsochromic shift for the absorption peak can indicate a drug–DNA interaction [41]. Fig. 6 exhibits the UV–vis spectra of the BNN-17 alone (a) and the dsDNA–BNN-17 mixtures (b–e). As can be seen from Fig. 6, the BNN-17 exhibited two absorption peaks at about 275 and 285 nm. The

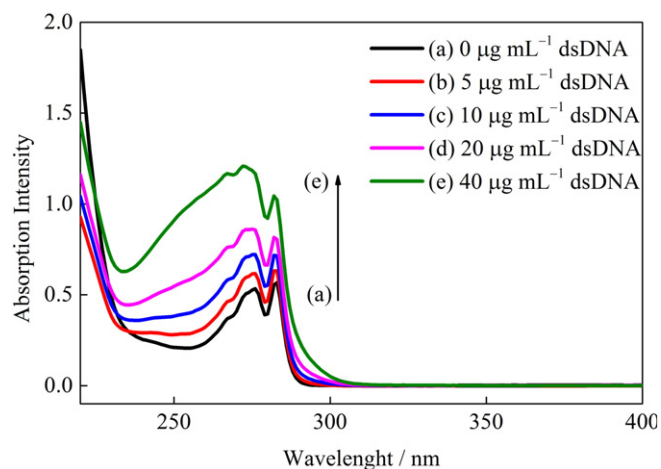


Fig. 6. UV–vis spectra of BNN-17 ($32.03 \mu\text{mol L}^{-1}$) in the absence and presence of dsDNA in the range of $5.0\text{--}40.0 \mu\text{g mL}^{-1}$.

hyperchromic effect in the absorption peaks of BNN-17 was observed with the addition of dsDNA ($5\text{--}40 \mu\text{g mL}^{-1}$) to the fixed concentration of the BNN-17 ($32.05 \mu\text{mol L}^{-1}$). In addition, no bathochromic shift was observed at the position of the maximum absorption of the BNN-17–dsDNA complexes. Thus, the absence of a bathochromic shift and hypochromic effect in the UV–vis spectra showed that the binding mode was not intercalative binding [42,43]. It is known that imidazole derivatives bind to the minor groove of dsDNA and show the AT sequence selectivity [44].

The binding constant (K) can be calculated from the equation based on the variations in the absorbance of the of BNN-17–dsDNA complexes:

$$\frac{A_0}{A - A_0} = \frac{\varepsilon_G}{\varepsilon_{\text{H-G}} - \varepsilon_G} + \frac{\varepsilon_G}{\varepsilon_{\text{H-G}} - \varepsilon_G} \times \frac{1}{K[\text{DNA}]} \quad (4)$$

where K is the binding constant; A_0 and A are the absorbance values of the drug and its complex with dsDNA, respectively, and ε_G and $\varepsilon_{\text{H-G}}$ are the absorption coefficients of the drug and the BNN-17–dsDNA complex, respectively. The binding constant, K , can be obtained from the intercept-to-slope ratio of the $A_0/(A - A_0)$ vs. $1/[\text{dsDNA}]$ plot. The value of K for the BNN-17–dsDNA interaction was calculated to be $3.27 \times 10^3 \text{ L mol}^{-1}$. Moreover, it was close to the value obtained from the DPV method ($2.9 \times 10^3 \text{ L mol}^{-1}$). The calculated values of K are in the order of 10^3 , which is significantly lower than that of the classic intercalation binding like the EtBr–DNA complex ($K = 1.4 \times 10^6 \text{ L mol}^{-1}$). This indicates that the interaction mode between the dsDNA and BNN-17 may be that of groove binding [45].

To confirm the interaction of the BNN-17 with the dsDNA immobilized at the GCE/P(AT) surface, the effect of the salt concentration on the guanine oxidation signal was investigated. DPVs were obtained in 0.5 mmol L^{-1} ABS (pH 4.8) containing different concentrations of NaCl ($5.0\text{--}40 \text{ mmol L}^{-1}$) (Fig. S2). As shown in Fig. S2, the peak current of the guanine hardly changed with the increasing salt concentration of the acetate buffer. The electrostatic interaction between the small molecule and the dsDNA is one of non-covalent binding, which served as an auxiliary mode to assist the intercalation and groove binding. If the electrostatic interaction occurs between the small molecule and dsDNA, the strength of the interaction decreases with an increase in the salt concentration in the solution [46,47]. The results indicated that there was no significant electrostatic binding between the BNN-17 and dsDNA.

3.7. Molecular docking

The docking method is an effective way to predict the correct binding mode and the interaction between the target and the ligand.

Table 1

Analytical characteristics for voltammetric determination of BNN-17 using DPV at GCE/P(AT)/dsDNA electrode.

Parameters	Obtained results
Potential applied (V)	0.80
Linearity range ($\mu\text{mol L}^{-1}$)	0.213–32.03
Sensitivity ($\mu\text{A } \mu\text{mol}^{-1} \text{ L}$)	–0.0105
Determination coefficient (R^2)	0.991
SE of slope	7.53×10^{-4}
SE of intercept	0.006
LOD ($\mu\text{mol L}^{-1}$)	0.063
LOQ ($\mu\text{mol L}^{-1}$)	0.210
RSD for repeatability	2.15% ($n = 7$)
RSD for reproducibility	3.17% ($n = 5$)

Targeting the minor groove of dsDNA through the binding of a small molecule is considered to be an important tool in the molecular recognition of a specific dsDNA sequence [48]. The spectroscopic results explained here were further confirmed by molecular docking studies that provide insight into the interaction of BNN-17 with the minor groove of dsDNA. According to the docking results, BNN-17 showed a hydrogen bond with the deoxythymidine, DT8 (the bond length was 1.87 Å between the NH hydrogen of the imidazole ring and the carbonyl oxygen of the thymine) and showed a π -sigma interaction with the deoxycytidine, DC9 (between the phenyl ring of the benzimidazole and the C-4 hydrogen of the deoxyribose) (Fig. 7). The free binding energy (ΔG) of the interaction between the BNN-17 and the dsDNA was estimated to be -4.75 kcal/mol. Furthermore, the binding constant, K , between the BNN-17 and the dsDNA obtained by UV-vis spectroscopic and electrochemical results were correlated with the free binding energy of the docked model. The basic formula of the binding constant and Gibbs free energy is [49]

$\Delta G = -RT \ln K$, where ΔG is the free energy, R is the gas constant (1.98 cal/mol/k), T is the temperature (298 K), and K is the binding constant which is calculated using the UV-vis spectroscopic results ($3.27 \times 10^3 \text{ M}^{-1}$) and the electrochemical results ($2.90 \times 10^3 \text{ M}^{-1}$). According to the UV-vis spectroscopic and electrochemical results, ΔG was calculated to be -4.78 and -4.70 kcal/mol, respectively. The free energy, ΔG , was calculated to be -4.78 kcal/mol. This value approximately matches the docked BNN-17 and the dsDNA model that is -4.75 kcal/mol. The docked model has a good correlation with our experimental results.

3.8. Interference study and storage stability

Interference studies were performed with various substances such as ascorbic acid, uric acid, *D*-glucose, *L*-cysteine, and dopamine. Fig. 8 shows the responses of the GCE/P(AT)/dsDNA electrode in a $0.032 \text{ mmol L}^{-1}$ BNN-17 solution (pH 4.8) before and after adding 0.1 mmol L^{-1} of these substances. The tolerance limit was defined as the maximum concentration of the interfering substance that caused

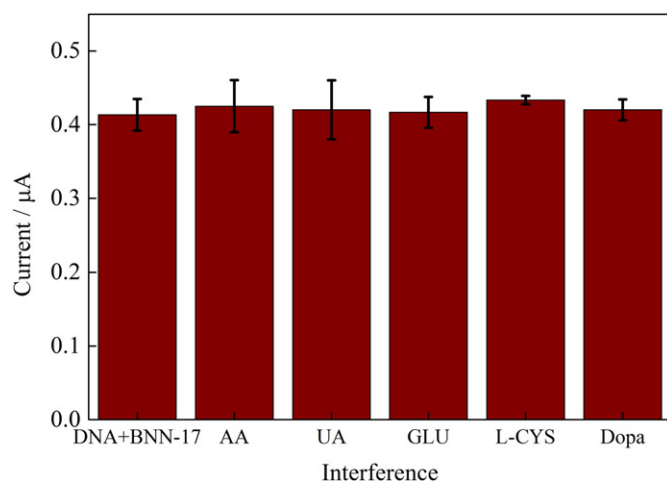


Fig. 8. Guanine peak currents of GCE/P(AT)/dsDNA for $0.032 \text{ mmol L}^{-1}$ BNN-17 in 0.5 mmol L^{-1} ABS (pH 4.8) containing 0.02 mmol L^{-1} NaCl before (dsDNA + BNN-17) and after adding of 0.01 mmol L^{-1} ascorbic acid (AA), uric acid (UA), *D*-glucose (D-GLU), *L*-cysteine (L-CYS), and dopamine (Dopa).

an error of $<5\%$ [35]. It can be seen that all these substances hardly caused any interference on the guanine oxidation current, which indicated the high selectivity of the recommended method for the BNN-17 determination. The storage stability of the modified electrode was also evaluated. The guanine oxidation response current decreased to 86.2% of initial value after 2 weeks and 75.4% remained after 3 weeks storage, showing a good long-term stability.

3.9. Serum sample analysis

To evaluate the analytical applicability of the proposed method, human serum samples were selected for the BNN-17 analysis. The

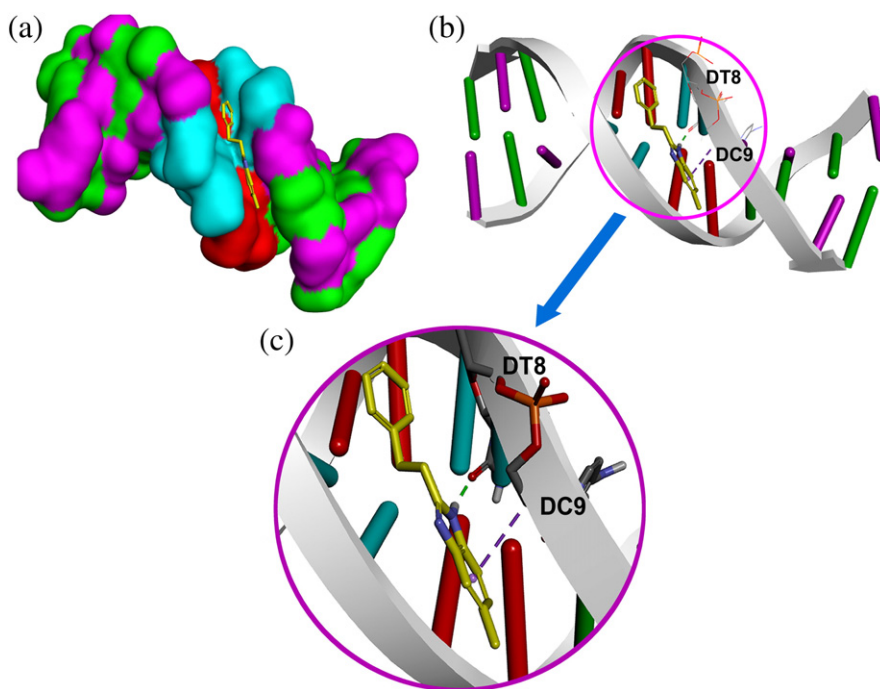


Fig. 7. (a) Docking overlay of BNN-17 (shown in stick representation and C atoms rendered in yellow) in DNA dodecamer (1BNA) surface area as parent colors: deoxyadenosine (DA) rendered in red, deoxyguanosine (DG) rendered in green, deoxycytidine (DC) rendered in purple, and deoxythymidine (DT) rendered in blue. (b) Docking position of BNN-17 in the minor groove of DNA. (c) A close-up view of the binding: BNN-17 showed hydrogen bond with the deoxythymidine DT8, between the NH hydrogen of imidazole ring and the carbonyl oxygen of the thymine and showed π -sigma interaction with the deoxycytidine DC9, between phenyl ring of benzimidazole and C-4 hydrogen of deoxyribose (hydrogen bond is shown as green dashed line, π -sigma interaction is shown as purple dashed line).

Table 2
Determination of BNN-17 in serum samples.

Sample no	Amount of added ($\mu\text{mol L}^{-1}$)	Amount of found ($\mu\text{mol L}^{-1}$)	Recovery (%)	RSD* (%)	Bias (%)
1	2.135	2.15	100.7	6.68	0.70
2	4.270	4.278	100.2	4.46	0.19
3	21.35	21.88	102.5	2.91	2.48

* Each value is the mean of three measurements.

recovery rates of the samples ranged between 100.2 and 102.5, and they are given in Table 2. The results indicated the applicability of the proposed electrochemical dsDNA biosensor based on the GCE/P(AT)/dsDNA electrode for the analysis of BNN-17 in human serum.

4. Conclusion

In the present study, a selective and sensitive electrochemical dsDNA biosensor based on a GCE/P(AT) electrode was constructed and used for the determination of BNN-17 for the first time. The P(AT)-film-modified GCE enhanced the electron transfer at the solution/electrode interface according to the results obtained by the CV and EIS methods using $\text{Fe}(\text{CN})_6^{3-/4-}$ as the redox probe. The interaction mechanism between the dsDNA and the BNN-17 was examined by electrochemical, spectroscopic, and molecular docking methods, and the results revealed that the BNN-17 bound to the dsDNA minor groove with the binding energies of -4.70 , -4.78 , and -4.75 kcal/mol, respectively. These values approximately match with each other. The proposed DNA biosensor has excellent applicability for the determination of BNN-17 in human serum samples. Moreover, the present method could contribute to understanding the interaction mechanism of benzimidazole compounds with dsDNA and lead to the design of new drug compounds.

Acknowledgment

This work was supported by the Ankara University Scientific Research Fund (BAP).

Appendix A. Supplementary data

Supplementary data to this article can be found online at <http://dx.doi.org/10.1016/j.jelechem.2016.06.028>.

References

- [1] M. Gaba, P. Gaba, D. Uppal, N. Dhingra, M.S. Bahia, O. Silakari, C. Mohan, Benzimidazole derivatives: search for GI-friendly anti-inflammatory analgesic agents, *Acta Pharm. Sin. B* 5 (2015) 337–342.
- [2] A.M. Mehranpour, M. Zahiri, Synthesis and characterization of new benzimidazole derivatives using 2-substituted 1,3-bis(dimethylamino)-trimethinium salts, *Tetrahedron Lett.* 55 (2014) 3969–3971.
- [3] A.A. El Rashedy, H.Y. Aboul-Enein, Benzimidazole derivatives as potential anticancer agents, *Mini- Rev. Med. Chem.* 13 (2013) 399–407.
- [4] G.L. Chen, L. Yang, T.C. Rowe, B.D. Halligan, K.M. Tewey, L.F. Liu, Nonintercalative antitumor drugs interfere with the breakage-reunion reaction of mammalian DNA topoisomerase II, *J. Biol. Chem.* 259 (1984) 13560–13566.
- [5] K. Tewey, T. Rowe, L. Yang, B. Halligan, L. Liu, Adriamycin-induced DNA damage mediated by mammalian DNA topoisomerase II, *Science* 226 (1984) 466–468.
- [6] J.L. Nitiss, Targeting DNA topoisomerase II in cancer chemotherapy, *Nat. Rev. Cancer* 9 (2009) 338–350.
- [7] S. Alper, Ö. Temiz Arpacı, E. Şener Aki, I. Yalçın, Some new bi- and ter-benzimidazole derivatives as topoisomerase I inhibitors, *II Farmaco* 58 (2003) 497–507.
- [8] B. Tolner, J.A. Hartley, D. Hochhauser, Transcriptional regulation of topoisomerase II α at confluence and pharmacological modulation of expression by bis-benzimidazole drugs, *Mol. Pharmacol.* 59 (2001) 699–706.
- [9] Q. Sun, B. Gatto, C. Yu, A. Liu, L.F. Liu, E.J. LaVoie, Synthesis and evaluation of Terbenzimidazoles as topoisomerase I inhibitors, *J. Med. Chem.* 38 (1995) 3638–3644.
- [10] G.J. Finlay, B.C. Baguley, Potentiation by phenylbisbenzimidazoles of cytotoxicity of anticancer drugs directed against topoisomerase II, *Eur. J. Cancer* 26 (1990) 586–589 (Oxford, England : 1990).
- [11] T.C. Rowe, G.L. Chen, Y.-H. Hsiang, L.F. Liu, DNA damage by antitumor Acridines mediated by mammalian DNA topoisomerase II, *Cancer Res.* 46 (1986) 2021–2026.
- [12] L.H. Fornander, L. Wu, M. Billeter, P. Lincoln, B. Nordén, Minor-groove binding drugs: where is the second Hoechst 33258 molecule? *J. Phys. Chem. B* 117 (2013) 5820–5830.
- [13] A.Y. Chen, C. Yu, A. Bodley, L.F. Peng, L.F. Liu, A new mammalian DNA topoisomerase I poison Hoechst 33342: cytotoxicity and drug resistance in human cell cultures, *Cancer Res.* 53 (1993) 1332–1337.
- [14] E. Oksuzoglu, B. Tekiner-Gulbas, S. Alper, O. Temiz-Arpaci, T. Ertan, I. Yildiz, N. Diril, E. Sener-Aki, I. Yalçın, Some benzoxazoles and benzimidazoles as DNA topoisomerase I and II inhibitors, *J. Enzyme Inhib. Med. Chem.* 23 (2008) 37–42.
- [15] M. Ligaj, M. Tichoniuk, D. Gwiazdowska, M. Filipiak, Electrochemical DNA biosensor for the detection of pathogenic bacteria *Aeromonas hydrophila*, *Electrochim. Acta* 128 (2014) 67–74.
- [16] G. Marrazza, G. Chiti, M. Mascini, M. Anichini, Detection of human apolipoprotein E genotypes by DNA electrochemical biosensor coupled with PCR, *Clin. Chem.* 46 (2000) 31–37.
- [17] V.C. Diculescu, A.M. Oliveira-Brett, In situ electrochemical evaluation of dsDNA interaction with the anticancer drug danusertib nitrenium radical product using the DNA-electrochemical biosensor, *Bioelectrochemistry* 107 (2016) 50–57.
- [18] G. Aydoğdu, G. Günendi, D.K. Zeybek, B. Zeybek, Ş. Pekyardımcı, A novel electrochemical DNA biosensor based on poly-(5-amino-2-mercapto-1,3,4-thiadiazole) modified glassy carbon electrode for the determination of nitrofurantoin, *Sensors Actuators B Chem.* 197 (2014) 211–219.
- [19] R.J. Geise, J.M. Adams, N.J. Barone, A.M. Yacynych, Electropolymerized films to prevent interferences and electrode fouling in biosensors, *Biosens. Bioelectron.* 6 (1991) 151–160.
- [20] B.D. Malhotra, A. Chaubey, S.P. Singh, Prospects of conducting polymers in biosensors, *Anal. Chim. Acta* 578 (2006) 59–74.
- [21] D.T. McQuade, A.E. Pullen, T.M. Swager, Conjugated polymer-based chemical sensors, *Chem. Rev.* 100 (2000) 2537–2574.
- [22] D. Koyuncu Zeybek, B. Demir, B. Zeybek, Ş. Pekyardımcı, A sensitive electrochemical DNA biosensor for antineoplastic drug 5-fluorouracil based on glassy carbon electrode modified with poly(bromocresol purple), *Talanta* 144 (2015) 793–800.
- [23] C. Wang, X. Zou, X. Zhao, Q. Wang, J. Tan, R. Yuan, Cu-nanoparticles incorporated overoxidized-poly(3-amino-5-mercapto-1,2,4-triazole) film modified electrode for the simultaneous determination of ascorbic acid, dopamine, uric acid and tryptophan, *J. Electroanal. Chem.* 741 (2015) 36–41.
- [24] S.B. Revin, S.A. John, Electrochemical marker for metastatic malignant melanoma based on the determination of l-dopa/l-tyrosine ratio, *Sensors Actuators B Chem.* 188 (2013) 1026–1032.
- [25] S.B. Revin, S.A. John, Electropolymerization of 3-amino-5-mercapto-1,2,4-triazole on glassy carbon electrode and its electrocatalytic activity towards uric acid, *Electrochim. Acta* 56 (2011) 8934–8940.
- [26] I. Oren, O. Temiz, I. Yalçın, E. Sener, A. Akin, N. Uçartürk, Synthesis and microbiological activity of 5(or 6)-methyl-2-substituted benzoxazole and benzimidazole derivatives, *Arzneimittelforschung* 47 (1997) 1393–1397.
- [27] I. Yildiz-Oren, I. Yalçın, E. Aki-Sener, N. Ucarturk, Synthesis and structure-activity relationships of new antimicrobial active multisubstituted benzazole derivatives, *Eur. J. Med. Chem.* 39 (2004) 291–298.
- [28] H.R. Drew, R.M. Wing, T. Takano, C. Broka, S. Tanaka, K. Itakura, R.E. Dickerson, Structure of a B-DNA dodecamer: conformation and dynamics, *Proc. Natl. Acad. Sci. U. S. A.* 78 (1981) 2179–2183.
- [29] G. Wu, D.H. Robertson, C.L. Brooks, M. Vieth, Detailed analysis of grid-based molecular docking: a case study of CDOCKER—A CHARMM-based MD docking algorithm, *J. Comput. Chem.* 24 (2003) 1549–1562.
- [30] Y. Liu, R. Yuan, Y. Chai, D. Tang, J. Dai, X. Zhong, Direct electrochemistry of horseradish peroxidase immobilized on gold colloid/cysteine/nafion-modified platinum disk electrode, *Sensors Actuators B Chem.* 115 (2006) 109–115.
- [31] J.-B. He, F. Qi, Y. Wang, N. Deng, Solid carbon paste-based amperometric sensor with electropolymerized film of 2-amino-5-mercapto-1,3,4-thiadiazole, *Sensors Actuators B Chem.* 145 (2010) 480–487.
- [32] J. Wang, Study of Electrode Reactions and Interfacial Properties, *Analytical Electrochemistry*, John Wiley & Sons, Inc., 2006 29–66.
- [33] L. Wang, L. Lin, B. Ye, Electrochemical studies of the interaction of the anticancer herbal drug emodin with DNA, *J. Pharm. Biomed. Anal.* 42 (2006) 625–629.
- [34] B. Dogan-Topal, B. Uslu, S.A. Ozkan, Voltammetric studies on the HIV-1 inhibitory drug Efavirenz: the interaction between dsDNA and drug using electrochemical DNA biosensor and adsorptive stripping voltammetric determination on disposable pencil graphite electrode, *Biosens. Bioelectron.* 24 (2009) 2358–2364.
- [35] A.A. Ensafi, P. Nasr-Esfahani, E. Heydari-Bafrooei, B. Rezaei, Determination of atropine sulfate using a novel sensitive DNA-biosensor based on its interaction on a modified pencil graphite electrode, *Talanta* 131 (2015) 149–155.
- [36] C.C. Chan, Analytical method validation: principles and practices, *Pharmaceutical Sciences Encyclopedia*, John Wiley & Sons, Inc., 2010
- [37] K.E. Erkkila, D.T. Odom, J.K. Barton, Recognition and reaction of metallointercalators with DNA, *Chem. Rev.* 99 (1999) 2777–2795.
- [38] M.T. Carter, M. Rodriguez, A.J. Bard, Voltammetric studies of the interaction of metal chelates with DNA. 2. Tris-chelated complexes of cobalt(III) and iron(II) with 1,10-phenanthroline and 2,2'-bipyridine, *J. Am. Chem. Soc.* 111 (1989) 8901–8911.
- [39] H. Nawaz, S. Rauf, K. Akhtar, A.M. Khalid, Electrochemical DNA biosensor for the study of ciprofloxacin-DNA interaction, *Anal. Biochem.* 354 (2006) 28–34.
- [40] B. Rafique, A.M. Khalid, K. Akhtar, A. Jabbar, Interaction of anticancer drug methotrexate with DNA analyzed by electrochemical and spectroscopic methods, *Biosens. Bioelectron.* 44 (2013) 21–26.

- [41] M. Rahban, A. Divsalar, A.A. Saboury, A. Golestani, Nanotoxicity and spectroscopy studies of silver nanoparticle: calf thymus DNA and K562 as targets, *J. Phys.Chem. C* 114 (2010) 5798–5803.
- [42] A. Subastri, C.H. Ramamurthy, A. Suyavaran, R. Mareeswaran, P. Lokeswara Rao, M. Harikrishna, M. Suresh Kumar, V. Sujatha, C. Thirunavukkarasu, Spectroscopic and molecular docking studies on the interaction of troxerutin with DNA, *Int. J. Biol. Macromol.* 78 (2015) 122–129.
- [43] S.U. Rehman, T. Sarwar, M.A. Husain, H.M. Ishqi, M. Tabish, Studying non-covalent drug–DNA interactions, *Arch. Biochem. Biophys.* 576 (2015) 49–60.
- [44] S.M. Nelson, L.R. Ferguson, W.A. Denny, Non-covalent ligand/DNA interactions: minor groove binding agents, *Mutat. Res. Fundam. Mol. Mech. Mutagen.* 623 (2007) 24–40.
- [45] S.S. Kalanur, U. Katrahalli, J. Seetharamappa, Electrochemical studies and spectroscopic investigations on the interaction of an anticancer drug with DNA and their analytical applications, *J. Electroanal. Chem.* 636 (2009) 93–100.
- [46] J.-H. Shi, J. Chen, J. Wang, Y.-Y. Zhu, Binding interaction between sorafenib and calf thymus DNA: Spectroscopic methodology, viscosity measurement and molecular docking, *Spectrochim. Acta A* 136, Part B (2015) 443–450.
- [47] L. Strekowski, B. Wilson, Noncovalent interactions with DNA: an overview, *Mutat. Res. Fundam. Mol. Mech. Mutagen.* 623 (2007) 3–13.
- [48] M.-C. Zhu, X.-T. Cui, F.-C. Zhao, X.-Y. Ma, Z.-B. Han, E.-J. Gao, Synthesis, characterization, and DNA interaction of novel Pt(II) complexes and their cytotoxicity, apoptosis and molecular docking, *RSC Adv.* 5 (2015) 47798–47808.
- [49] S. Charak, R. Mehrotra, Structural investigation of idarubicin–DNA interaction: spectroscopic and molecular docking study, *Int. J. Biol. Macromol.* 60 (2013) 213–218.